

## Supplemental Material

**Figure S1.** Sequence alignment between GSNOR isozymes from *Chlamydomonas reinhardtii*

**Figure S2.** Primary and secondary structure alignment of plant and non-plant GSNORs

**Figure S3.** Structural analysis of CrGSNOR1

**Figure S4.** Cofactor and substrate binding sites in CrGSNOR1

**Figure S5.** Catalytic zinc movement and reversible association to Glu71

**Figure S6.** Stabilization of the water molecule involved in the catalytic zinc coordination sphere

**Figure S7.** Linear dependence of CrGSNOR1 activity on protein concentration

**Figure S8.** Biochemical properties of CrGSNOR1

**Figure S9.** Time-dependent mass spectrometry analyses of CrGSNOR1 treated with N-ethylmaleimide

**Figure S10.** Affinity purification of Biotin-maleimide derivatized peptides of CrGSNOR1

**Figure S11.** Cysteine 272 of CrGSNOR1 is unreactive toward Biotin-maleimide alkylation

**Figure S12.** Far-UV CD spectra reveal that secondary structures of CrGSNOR1 are not affected by thiol-based redox modifications

**Figure S13.** Electron density and interactions of S-nitrosylated Cys244 in CrGSNOR1 upon treatment with GSNO

**Figure S14.** Flexible and disordered regions in algae and plant GSNORs

**Table S1.** X-ray data collection and refinement statistics of CrGSNOR1 structures

**Table S2.** Secondary structure of CrGSNOR1



# Figure S2

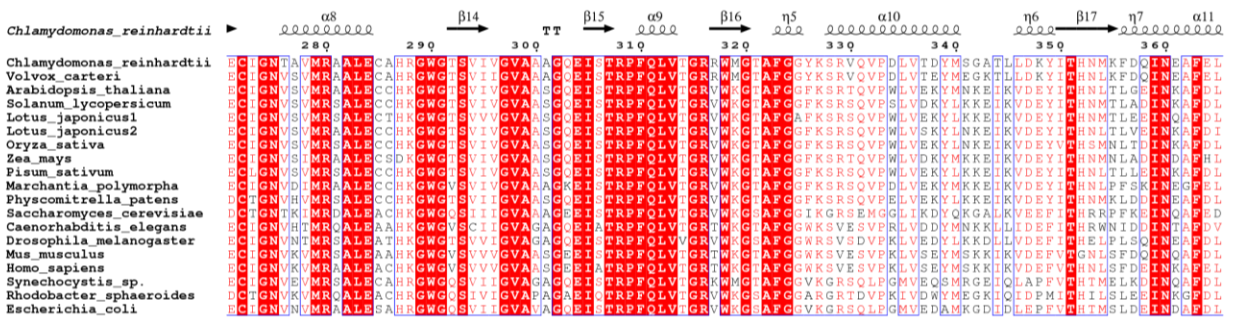
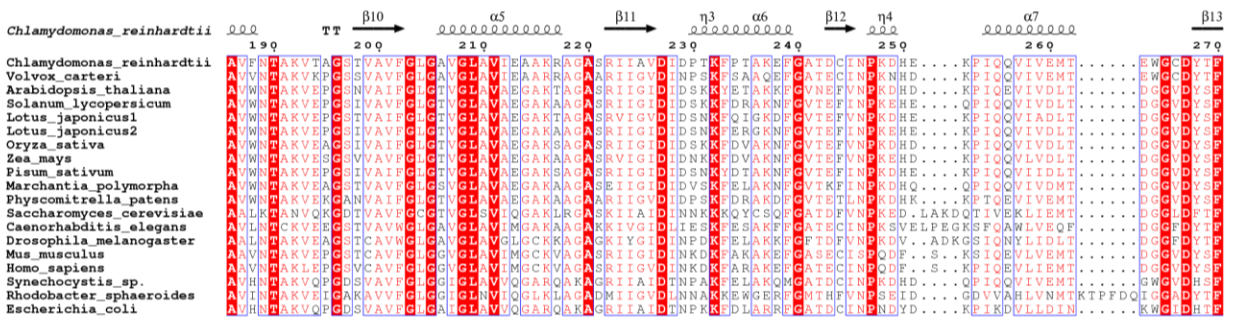
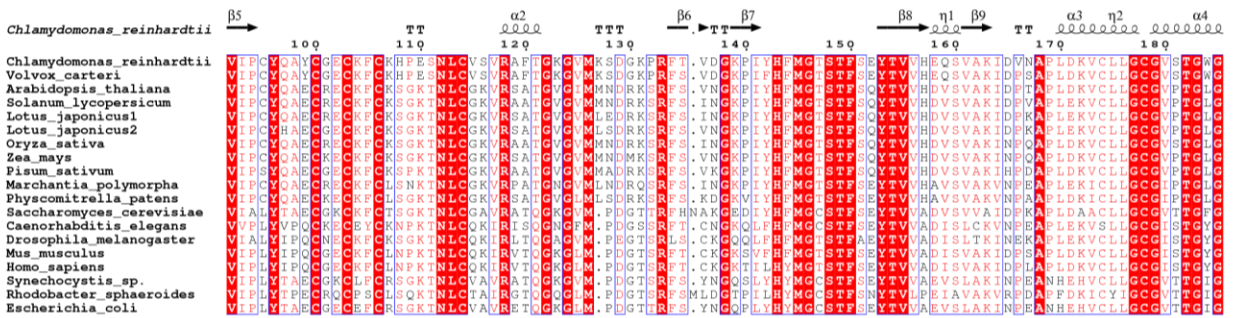
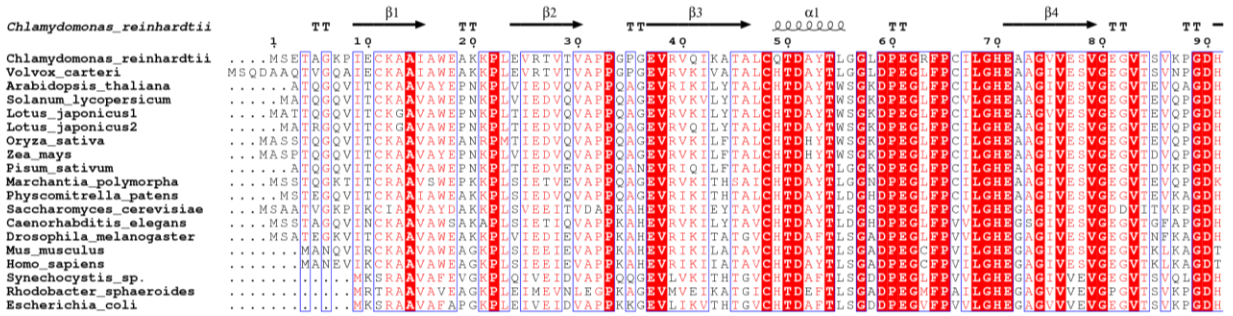


## **Figure S2. Primary and secondary structure alignment of plant and non-plant GSNORs**

The alignment was performed as described for Figure 2 using the sequence and the structure of CrGSNOR1 (this work) and GSNORs from other organisms. The conserved residues are shown in red background; blue boxes represent conserved amino acid stretches (>70%). Residues with similar physico-chemical properties are indicated in red.  $\alpha$ -helices,  $\beta$ -strands and 310-helices are marked with  $\alpha$ ,  $\beta$ ,  $\eta$  respectively.  $\beta$ -turns and  $\alpha$ -turns are represented by TT and TTT, respectively.

# Figure S3

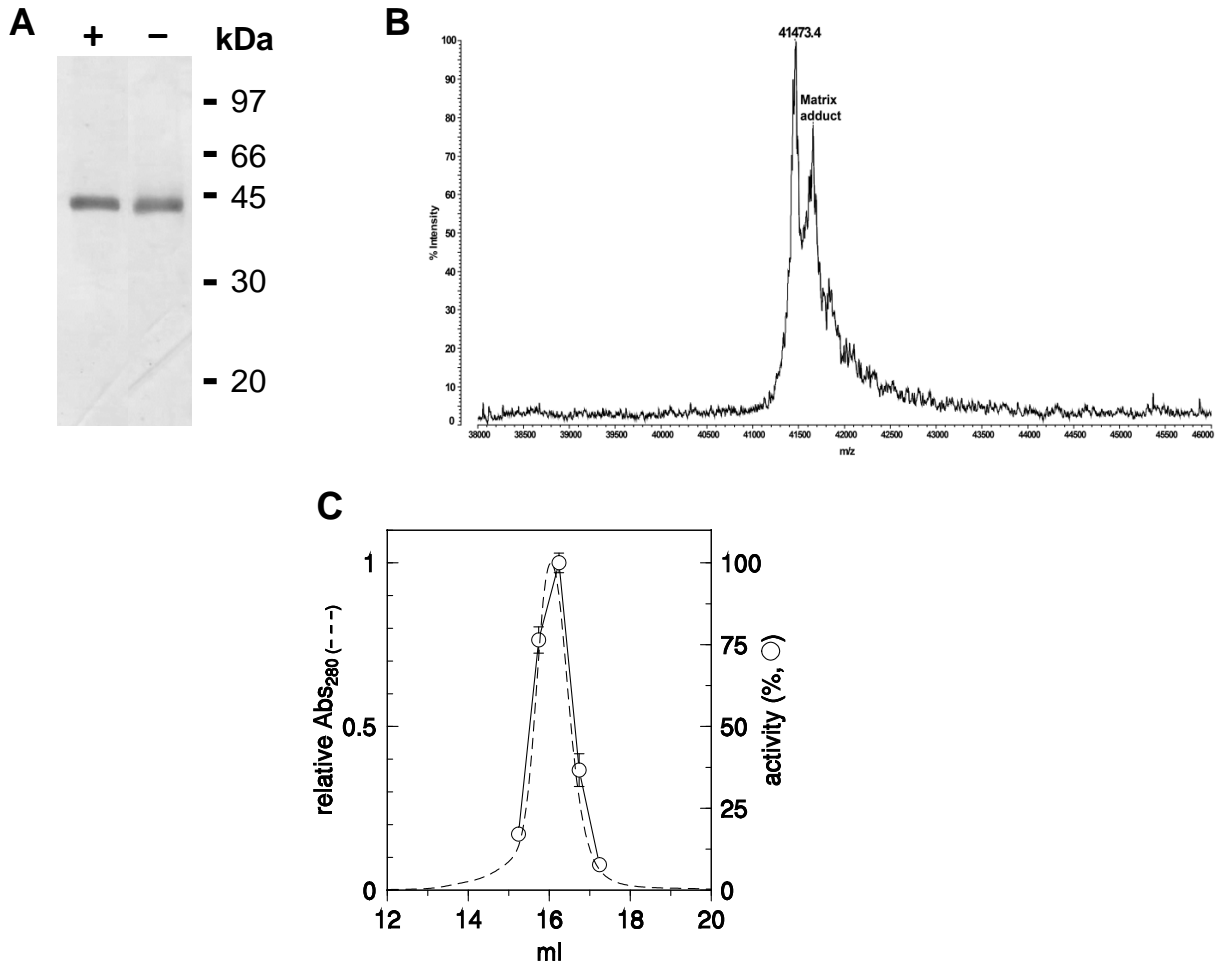


## Figure S3. Structural analysis of CrGSNOR1

(A) SDS-PAGE of recombinant CrGSNOR1. Sample proteins (2  $\mu$ g) were separated by 12% polyacrylamide gel under reducing (+) or non-reducing (-) conditions and stained with Coomassie Brilliant Blue. (B) Matrix-assisted laser desorption/ionization mass spectrum of intact protein (experimental mass of 41773.4 Da). The peak labelled "Matrix adduct" correspond to recombinant CrGSNOR1 with a sinapinic acid adduct. (C) Gel filtration elution profile of CrGSNOR1 (dashed black line). The columns were calibrated with globular protein markers (ferritin, 440 kDa; aldolase, 156 kDa; ovalbumin, 43 kDa; and chymotrypsinogen, 25 kDa). The activity of elution peak containing fractions was measured using GSNO and NADH as substrates (open circles). Data are represented as mean  $\pm$  SD (n = 3).

## Figure S4

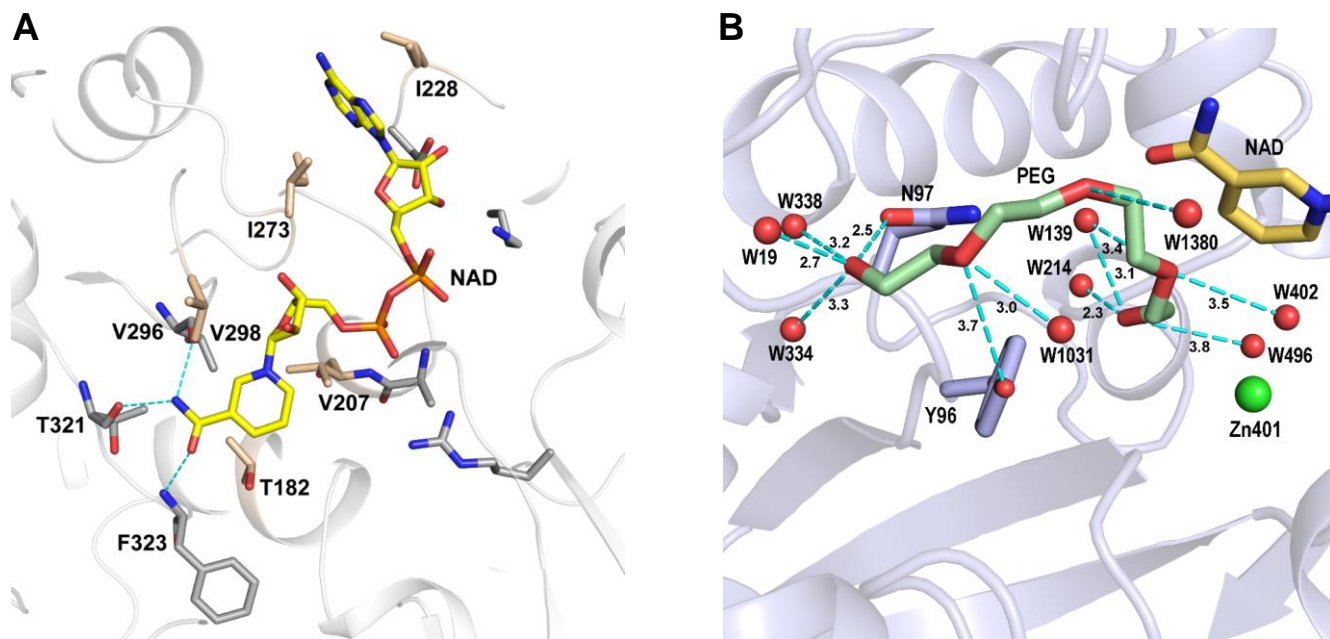


### Figure S4. Cofactor and substrate binding sites in CrGSNOR1

(A) Hydrophobic and hydrogen bond interactions of NAD<sup>+</sup> adenine and nicotinamide rings, with protein residues. (B) In all subunits of NAD<sup>+</sup>-CrGSNOR1 structure, a PEG molecule coming from the crystallization solution occupies the substrate-binding site. It is stabilized by hydrogen bonds with Tyr96, Gln97, NAD<sup>+</sup>, and several water molecules, but it does not contribute to the coordination of the catalytic zinc ion. The rotation of Tyr96 with respect to its position in apo-structure is required to accommodate PEG.



## Figure S5

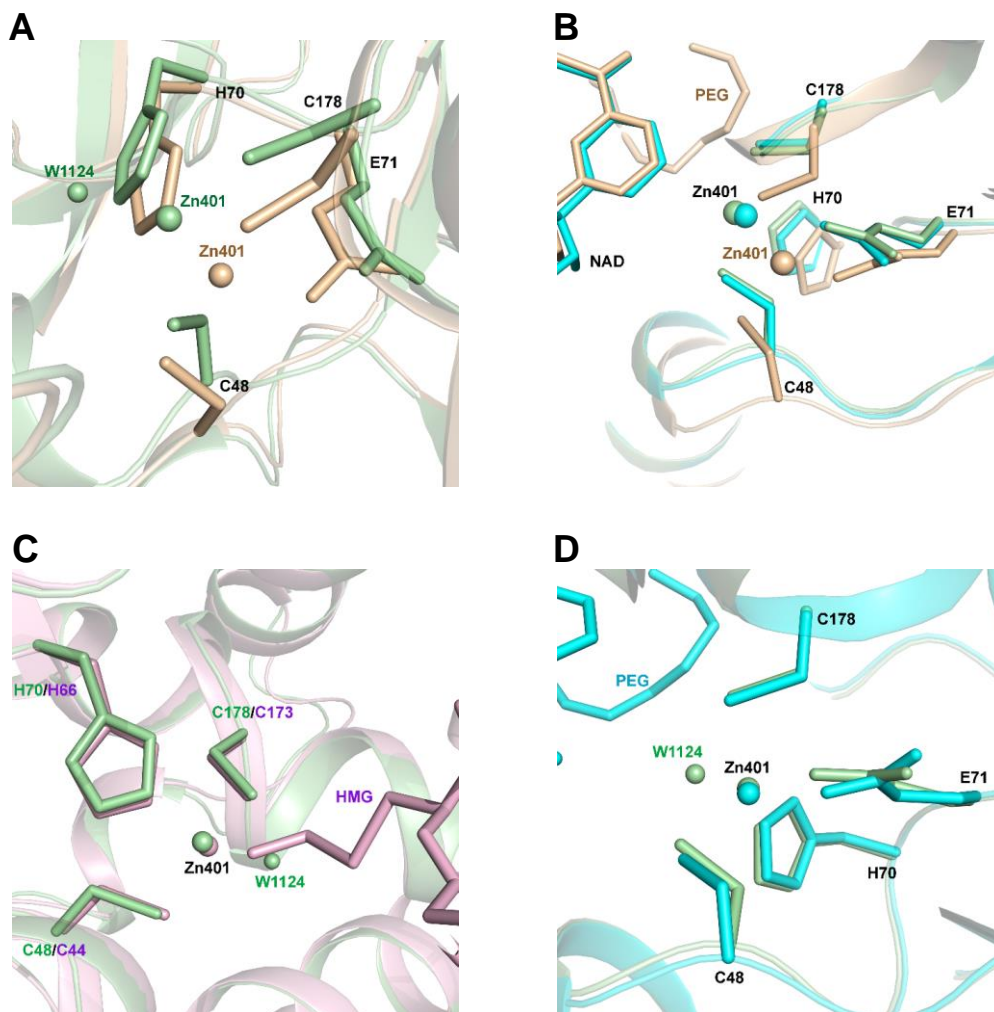


### Figure S5. Catalytic zinc movement and reversible association to Glu71

(A) The superimposition between the A subunit of NAD<sup>+</sup>-CrGSNOR1 (wheat) and F subunit of apo-CrGSNOR1 (pale green) shows that in the absence of the cofactor the catalytic zinc ion moves away from Glu71 and toward the water molecule coordinating it and located in the opposite direction with respect to Glu71. Conversely, when the cofactor binds to the enzyme the zinc ion moves toward Glu71. This is in agreement to what already observed in tomato and human (Hs) GSNORs (23, 66). (B) The superimposition between A (wheat) and F (pale cyan) subunits of NAD<sup>+</sup>-CrGSNOR1 shows that in this last subunit even if the cofactor is bound to the enzyme, the catalytic zinc is located far from Glu71 toward the substrate-binding site where a PEG molecule is observed. Moreover, it superimposes to the metal ion in F subunit (pale green) of apo-CrGSNOR1. (C) The superimposition between F subunit (pale green) of apo-CrGSNOR1 and A subunit (light pink) of HsGSNOR complexed with NADH and the substrate S-(hydroxymethyl)glutathione (HMGSH) (68) shows that in the absence of the cofactor the catalytic zinc ion occupies the same position observed when the substrate binds to the enzyme. (D) The superimposition between the A subunits of apo-CrGSNOR1 (light blue) and NAD<sup>+</sup>-CrGSNOR1 (wheat) shows that in the absence of the cofactor the catalytic zinc ion is at a coordination-distance from Glu71, as observed in the holo-structure.

# Figure S6

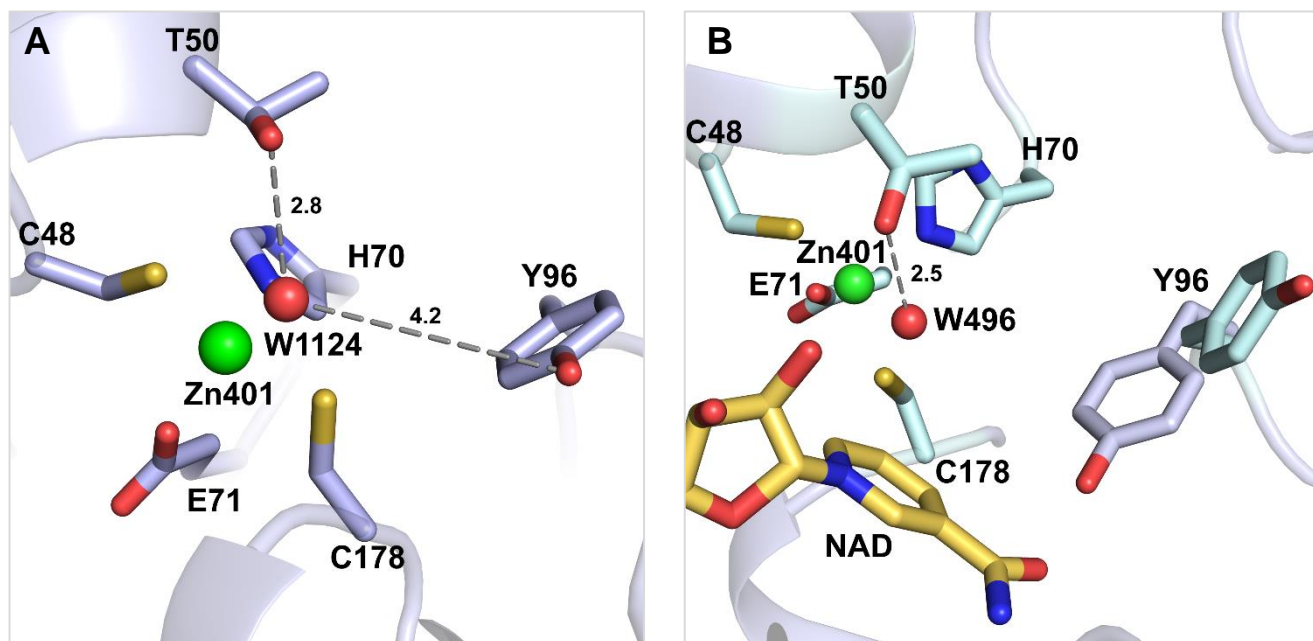


**Figure S6. Stabilization of the water molecule involved in the catalytic zinc coordination sphere.**

(A) The F subunit of apo-CrGSNOR1 structure shows a water molecule participating to the coordination of the catalytic zinc and stabilized by hydrogen-bonds with Thr50 and Tyr96. This water is observed in all other subunits of apo-structure (B) The B subunit of NAD<sup>+</sup>-CrGSNOR1 structure, shows that the water molecule is in close proximity of the catalytic zinc ion and is stabilized by Thr50. However, it loses the stabilization from the hydroxyl group of Tyr96, which is rotated compared to the apo-form, shown in grey sticks. An analogous situation is observed in D subunit of NAD<sup>+</sup>-structure, while in the remaining subunits the water molecule is not found.



## Figure S7

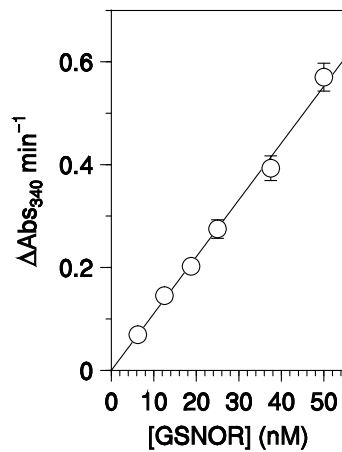


### Figure S7. Linear dependence of CrGSNOR1 activity on protein concentration

CrGSNOR1 activity was monitored under standard conditions (0.4 mM GSNO and 0.2 mM NADH) using variable amount of protein concentration. Data are expressed as Abs340/min and represented as mean  $\pm$  SD (n = 3).

## Figure S8

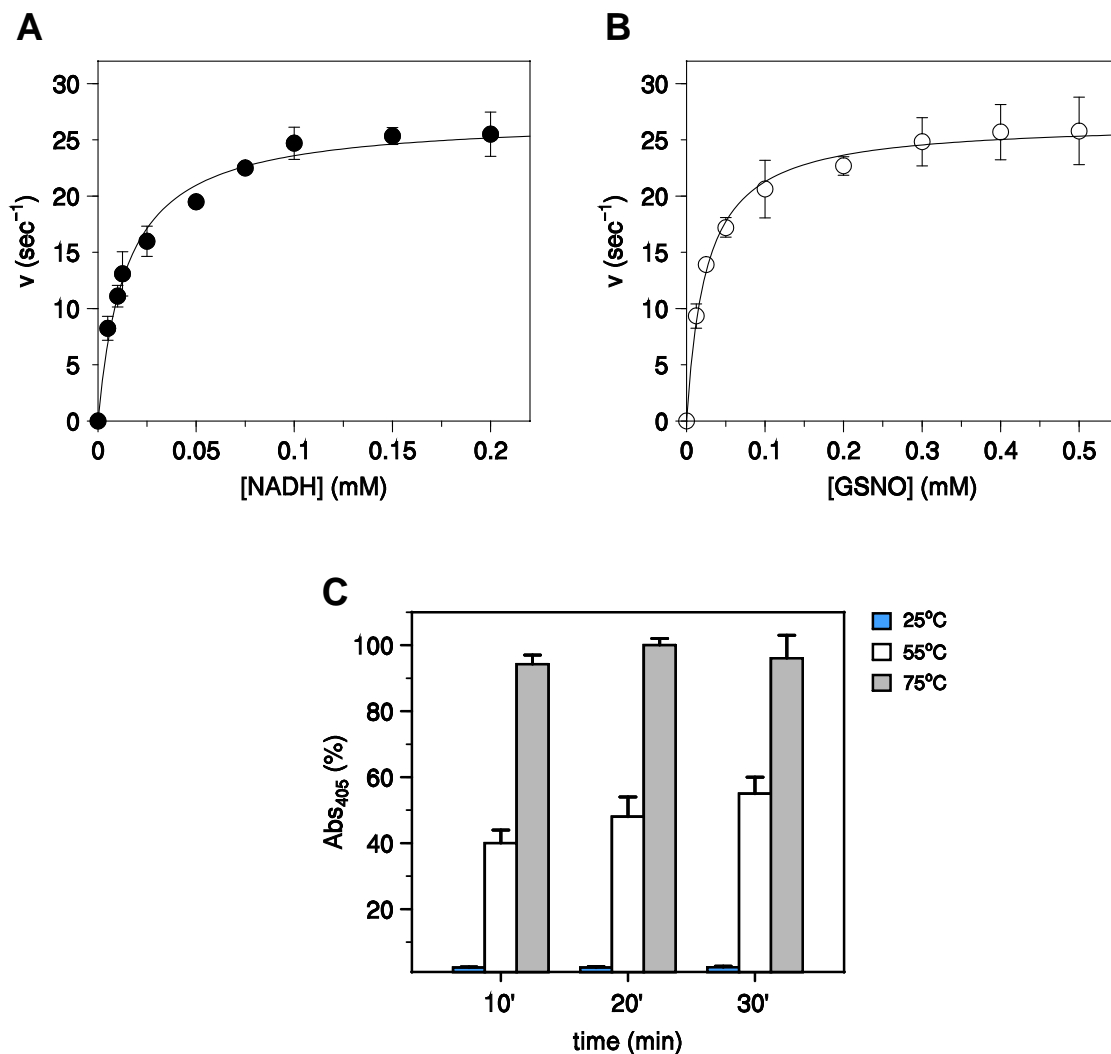


### Figure S8. Biochemical properties of CrGSNOR1

(A) Michaelis-Menten plot of variations of apparent velocity ( $v$ ,  $\text{sec}^{-1}$ ) versus [NADH]. CrGSNOR1 activity was assayed in the presence of 0.4 mM GSNO and varying NADH concentrations. Turnover represents moles of NADH oxidized  $\text{sec}^{-1}$  by 1 mole of CrGSNOR1. (B) Michaelis-Menten plot of variations of apparent velocity ( $v$ ,  $\text{sec}^{-1}$ ) versus [GSNO]. CrGSNOR1 activity was assayed in the presence of 0.2 mM NADH and varying GSNO concentrations. Turnover represents moles of NADH oxidized  $\text{sec}^{-1}$  by 1 mole of CrGSNOR1. For panels a-b, the apparent kinetic parameters were calculated using only nonlinear curve fit of the data sets. Data are represented as mean  $\pm$  SD ( $n = 3$ ). (C) Turbidity measurements were carried out at 405 nm by following incubation of CrGSNOR1 samples at 25 °C (white bars), 55 °C (grey bars) or 75 °C (black bars) at the indicated times. Data are represented as mean percentage  $\pm$  SD ( $n = 3$ ) of maximal turbidity measured at 75 °C after 30 min incubation. The Abs<sub>405</sub> of protein samples incubated at 25 °C (white bars) were negligible and corresponds to the absorbance of the buffer alone (30 mM Tris-HCl, pH 7.9).

## Figure S9

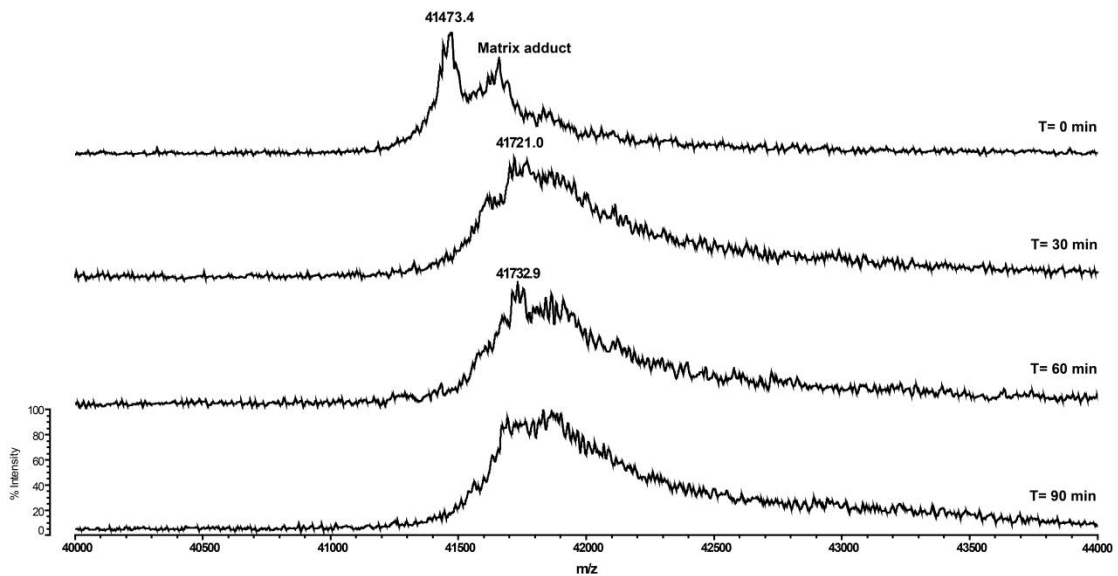


### Figure S9. Time-dependent mass spectrometry analyses of CrGSNOR1 treated with N-ethylmaleimide

Recombinant CrGSNOR1 was incubated in the presence of 1mM NEM. At indicated time points, protein samples were withdrawn and analyzed by MALDI-TOF MS to assess the number of alkylated cysteines. For each alkylated cysteine, the molecular mass of CrGSNOR1 is shifted by +125 Da compared to the native protein (41473.4 Da). The peak labelled "Matrix adduct" correspond to CrGSNOR1 with a sinapinic acid adduct. The y-axis is equal for all mass spectra acquired at times 0, 30, 60, and 90 min, and only indicated in the bottom spectrum.

## Figure S10

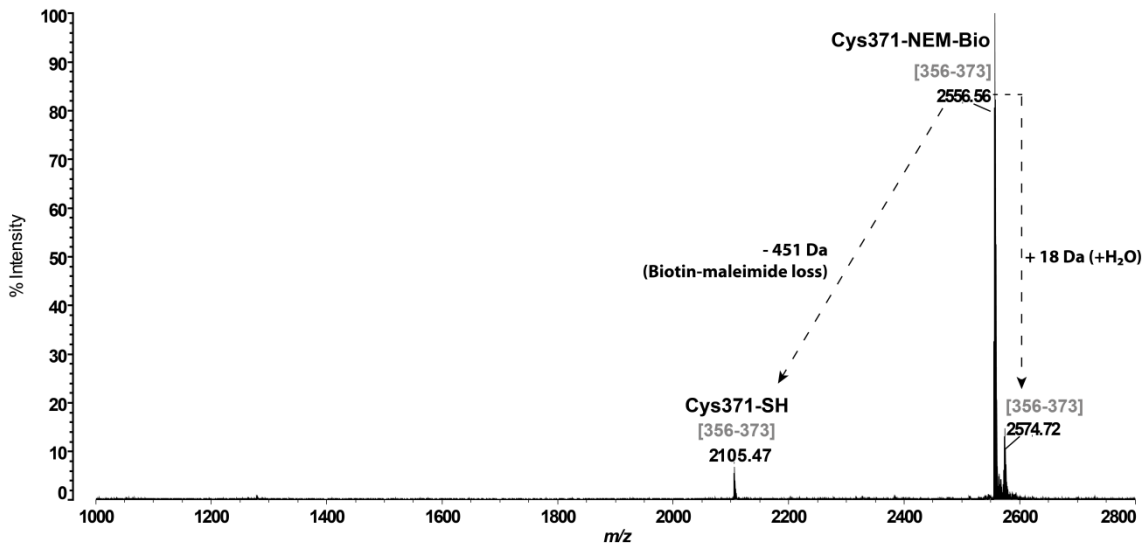


### Figure S10. Affinity purification of Biotin-maleimide derivatized peptides of CrGSNOR1

Recombinant CrGSNOR1 was incubated in the presence of 1mM Biotin-maleimide for 20 min and then trypsin digested. Biotinylated cysteinyl peptides were purified by affinity chromatography onto a monomeric avidin column and eluted under acidic conditions. After vacuum concentration, purified peptides were analyzed by MALDI-TOF MS. Peaks corresponding to ring-opening of the maleimide group into maleic amide (+H<sub>2</sub>O) as well as the loss of biotin-maleimide were observed under our acidic elution conditions. Sequence of peptides belonging to CrGSNOR1 is indicated in brackets (numbering according to the Figure 2).

# Figure S11

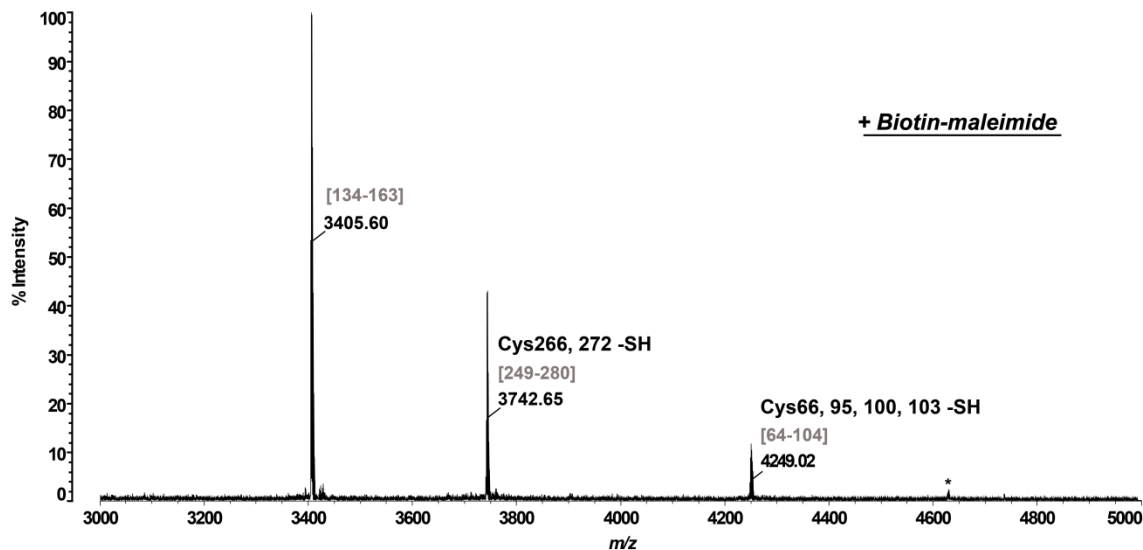


## Figure S11. Cysteine 272 of CrGSNOR1 is unreactive toward Biotin-maleimide alkylation

Recombinant CrGSNOR1 was incubated in the presence of 1 mM Biotin-maleimide for 20 min and then trypsin digested. The peptide mixture was analyzed by MALDI-TOF MS. Cysteinyl peptides in the mass range  $m/z$  3000-5000 are found exclusively as free thiols. Sequence of peptides belonging to CrGSNOR1 is indicated in brackets (numbering according to the Figure 2). The mass of the peak marked with an asterisk cannot be determined precisely but it can most likely be related to the peptide [72-115].

## Figure S12

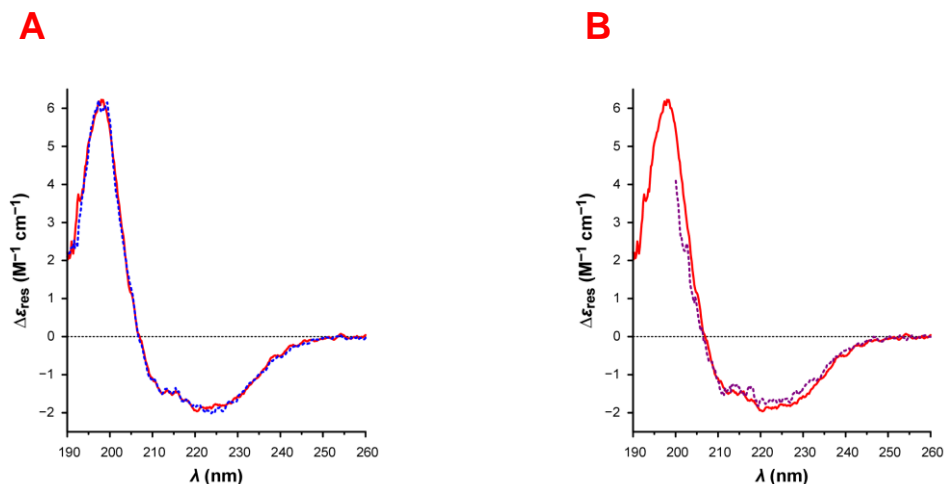


**Figure S12. Far-UV CD spectra reveal that secondary structures of CrGSNOR1 are not affected by thiol-based redox modifications**

(A) Far-UV CD spectra of CrGSNOR1 before (red solid line) and after (blue dotted line) treatment with  $H_2O_2$ . (B) Far-UV CD spectra of CrGSNOR1 before (red solid line) and after (purple dotted line) treatment with GSNO. For experimental details, see “Material and Methods” section.



## Figure S13

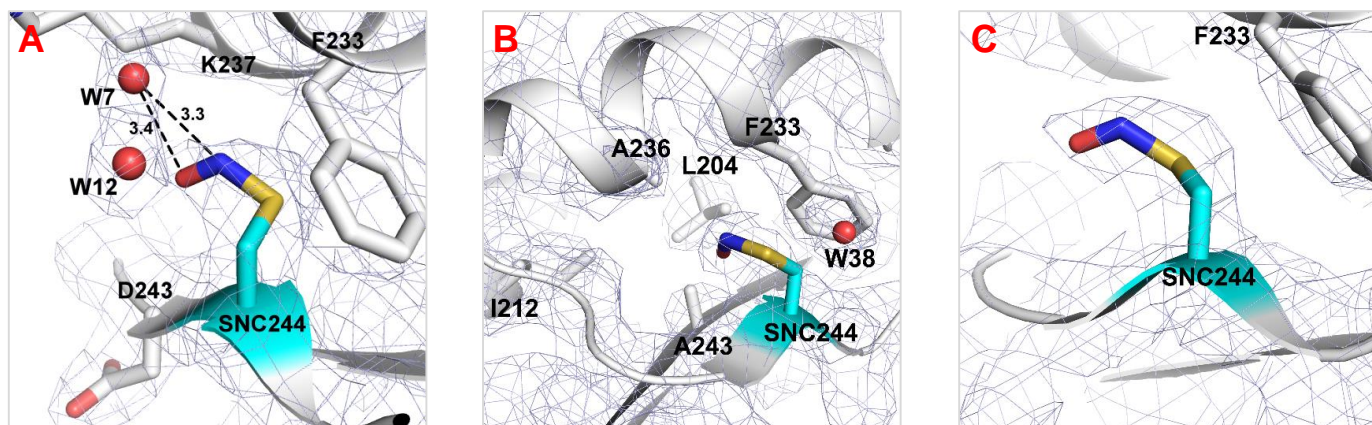


### Figure S13. Electron density and interactions of S-nitrosylated Cys244 in CrGSNOR1 upon treatment with GSNO

$2F_o - F_c$  electron density map (contoured at  $1\sigma$ ) and interactions (up to 4.0 Å) of nitrosylated Cys244 in (A) chain B; (B) chain A; (C) chains C, D and F of CrGSNOR1 structure. In chain B the nitrosothiol forms two hydrogen bonds with a water molecule.

## Figure S14

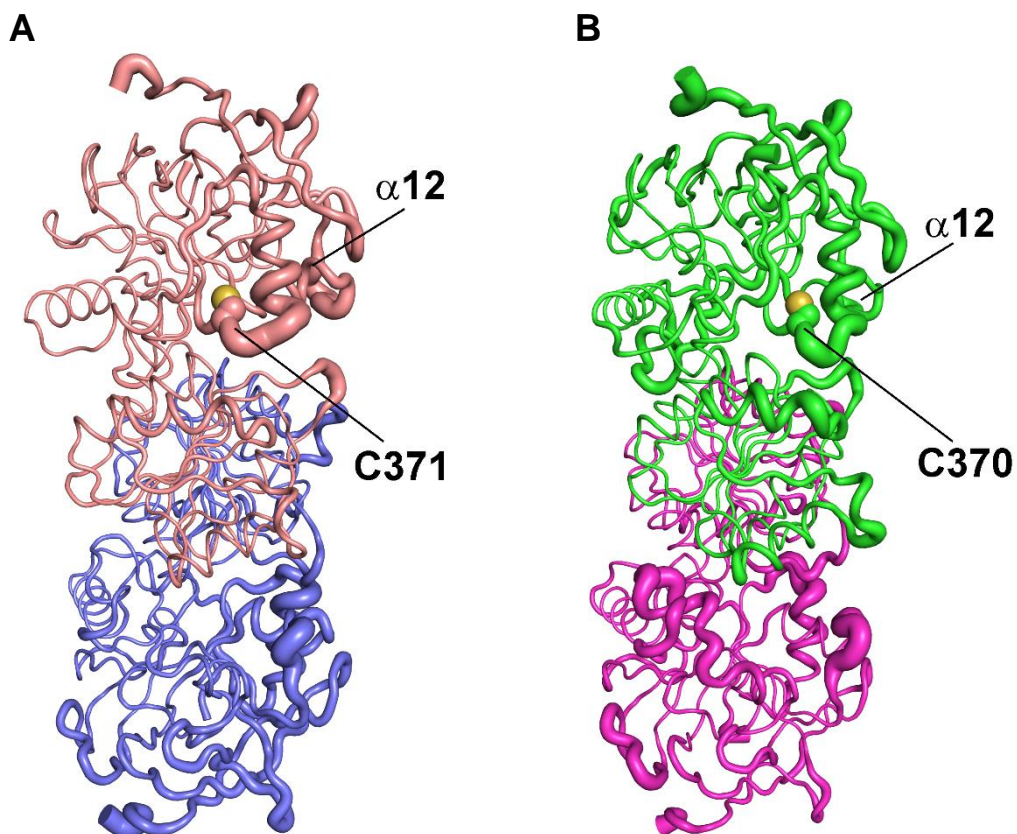


### Figure S14. Flexible and disordered regions in algae and plant GSNORs.

C<sub>α</sub> trace of (A) CrGSNOR1 and (B) AtGSNOR. The trace thickness is proportional to the atomic B factor. Cys371/370 in algae and plant enzymes, respectively, are represented as sphere. Helix  $\alpha 12$  is indicated in both enzymes.

**Table S1. X-ray data collection and refinement statistics of CrGSNOR1 structures**

	<b>Apo</b>	<b>NAD<sup>+</sup></b>	<b>NAD<sup>+</sup>/GSNO</b>
<i>Data collection</i>			
Unit cell (Å)	77.83 143.00 206.17 90.00 90.00 90.00	77.75 142.72 206.59 90.00 90.00 90.00	78.39 143.29 206.27 90.00 90.00 90.00
Space group	P2 <sub>1</sub> 2 <sub>1</sub> 2 <sub>1</sub>	P2 <sub>1</sub> 2 <sub>1</sub> 2 <sub>1</sub>	P2 <sub>1</sub> 2 <sub>1</sub> 2 <sub>1</sub>
Resolution range* (Å)	56.97 – 1.80 (1.83 – 1.80)	48.56 – 2.30 (2.34 – 2.30)	48.62 – 2.90 (3.06 – 2.90)
Unique reflections*	208518 (9027)	102418 (4861)	52231 (7444)
Completeness* (%)	98.1 (86.8)	99.7 (96.9)	99.7 (99.0)
R <sub>merge</sub> *	0.066 (0.507)	0.133 (0.704)	0.118 (0.536)
CC <sub>1/2</sub> *	0.998 (0.686)	0.988 (0.655)	0.986 (0.733)
I/σ(I) *	13.9 (1.9)	8.3 (2.2)	8.1 (2.1)
Multiplicity*	5.0 (2.7)	4.2 (3.9)	3.7 (3.5)
<i>Refinement</i>			
Resolution range* (Å)	56.97 – 1.80 (1.82 – 1.80)	48.58 – 2.30 (2.33 – 2.30)	48.53 – 2.90 (2.93 -2.90)
Reflection used	208409 (11305)	102297 (5959)	52134 (3133)
R/R <sub>free</sub>	0.173/0.205	0.178/0.226	0.180/0.257
rmsd from ideality (Å, °)	0.009, 0.912	0.004, 0.668	0.010, 1.038
<i>N° atoms</i>			
Non-hydrogen atoms	19327	18798	17275
Protein atoms	16973	16963	16950
Zn ions	12	12	12
Solvent molecules	2249	1453	48
Hetero atoms	93	370	277
<i>B value (Å<sup>2</sup>)</i>			
Mean	24.1	31.7	37.0
Wilson	13.6	22.2	30.7
Protein atoms	23.1	31.3	36.9
Zn ions	19.1	33.4	43.2
NAD <sup>+</sup>	/	29.1	51.0
Solvent molecules	31.3	35.2	21.1
Hetero atoms	32.9	39.1	61.0
<i>Ramachandran plot (%)<sup>§</sup></i>			
Most favoured	97.5	96.7	93.5
Allowed	2.3	3.0	6.1
Disallowed	0.2	0.3	0.4

\*Values in parentheses refer to the last resolution shell

§As defined by MolProbity (65)

**Table S2. Secondary structure of CrGSNOR1**

Secondary structure of CrGSNOR1 before and after treatment with H<sub>2</sub>O<sub>2</sub>, as determined by CD spectroscopic analysis; data obtained on the crystal structure are reported for comparison (experimental details are reported in the “Material and Methods” section).

<b>Structure</b>	<b>Before</b>	<b>After</b>	<b>Crystal</b>
Helices	26.1%	26.5%	28.7%
- <i>regular</i>	15.3%	15.4%	10.8%
- <i>distorted</i>	10.8%	11.1%	17.9%
Strands	29.7%	29.6%	23.4%
- <i>regular</i>	20.9%	20.9%	14.1%
- <i>distorted</i>	8.8%	8.7%	9.3%
Turns	18.6%	16.9%	15.3%
Unordered	25.6%	27.0%	32.6%